10th World Congress on Structural and Multidisciplinary Optimization
May 19 -24, 2013, Orlando, Florida, USA

Generating 3D Topologies with Multiple Constraints on the GPU

Krishnan Suresh

University of Wisconsin, Madison, USA, suresh@engr.wisc.edu

1. Abstract
The objective of this paper is to demonstrate a topology optimization method that can handle multiple constraints. The method relies on the concept of topological sensitivity that captures the first order change in any quantity of interest to a topological change. Specifically, in this paper, the topological sensitivity field for each of constraints is first computed. These fields are then dynamically combined to result in a single topological level-set. Finally, by relying on a fixed-point iteration, the topological level-set leads to optimal topologies (with decreasing volume fractions) that satisfy the constraints. Since the method relies on an assembly-free finite-element analysis, it is parallelization-friendly, and can be easily ported to the GPU, as demonstrated through examples in 3D.

2. Keywords: Topology optimization, GPU, constraints, sensitivity.

3. Introduction
Topology optimization plays an important role in structural design today; see [1] and [2] for a review. In this paper, we consider topology optimization problems with numerous displacement and stress constraints:

$$\begin{aligned} &\underset{\Omega \subset D}{Min}\, v \\ &\delta \le \delta_{allowed} \\ &\sigma \le \sigma_{allowed} \\ &Ku = f \end{aligned} \tag{1}$$

where:

$$\begin{aligned} &u: \text{ Finite element displacement field} \\ &K: \text{ Finite element stiffness matrix} \\ &f: \text{ External force vector (due to a point force)} \\ &\delta: \text{ Displacement at point of force application} \\ &\Omega: \text{ Topology to be computed} \\ &v: \text{ Volume of the topology} \\ &D: \text{ Region within which the topology must lie} \\ &\sigma: \text{ von Mises Stress} \end{aligned} \tag{2}$$

The most popular topology optimization method today is Solid Isotropic Material with Penalization (SIMP), where pseudo-density variables are used to define the evolving topology [3]. However, in the presence of low-density elements, SIMP can lead to ill-conditioned matrices that can pose serious computational challenges while solving the above problem. Therefore, a topological sensitivity [4] based level-set method is proposed in this paper. Since the resulting stiffness matrices are well-conditioned, simple iterative solvers, such as Jacobi-preconditioned conjugate gradient, are highly effective.

4. Literature Review
Topology optimization methods can broadly be classified into two distinct types: SIMP and level-set. A common challenge to both strategies is resolving the point-wise stress constraints in Equation (1), i.e., it is generally impossible to satisfy stress constraints at all points within the domain. Therefore, in a finite element implementation, the element-stresses are typically handled via one of the following methods: (1) via the p-norm [5], (2) Kreisselmeier− Steinhauser function [6], (3) potentially active constraints [7], and (4) global/local penalization [8]. The equivalence of some of these measures and their justification is discussed, for example, in [9]. Later in this paper, we shall exploit the p-norm global measure. Alternately, active-set methodologies have also been proposed where a finite number of elements with the highest stress states are chosen to be active during a given iteration [10], [11].

Solid Isotropic Material with Penalization (SIMP)

As stated earlier, the most popular topology optimization strategy today is SIMP where pseudo-densities are assigned to finite-elements, and then optimized to meet the desired objective [3]. The primary advantage of SIMP

is that it is well-developed, but the 'singularity-problem' associated with zero-density elements require careful treatment, for example through epsilon-methods [12], [13]. Secondly, the ill-conditioning of the stiffness matrices, once again due to the low-density elements, can lead to high computational costs for iterative solvers [14], [15]. Additional challenges including stress-ambiguity and accuracy over gray-elements are identified and discussed in [16].

One of the earliest implementation of SIMP for stress-constrained topology optimization was reported in [17], where the authors addressed instability and singularity issues via a weighted combination of displacement and global stress measure. Such concepts continue to play an important role today. In [18], the authors proposed a framework to design the material distribution of functionally graded structures with a tailored Von Mises stress field. In [6], the authors studied the weight minimization problems with global or local stress constraints, in which the global stress constraints are defined by the Kreisselmeier− Steinhauser function. In [13], to resolve the stress singularity phenomenon, a SIMP-motivated stress definition was used. In addition, the author used the restriction method with a density filter for length scale control. Finally, a global/regional stress measure combined with an adaptive normalization scheme to control the local stress level. The mixed finite element method (FEM) was proposed for stress-constrained topology optimization, to alleviate the challenges posed by displacement-based FEM [19]. More recently, the authors of [20] proposed a conservative global stress measure, and the objective function was constructed using the relationship between mean compliance and von Mises stress; the authors used a SIMP-based mesh-independent framework. In [10] Drucker–Prager failure criterion is considered within the SIMP framework to handle materials with different tension and compression behaviors; a stress-relaxation scheme is proposed to handle the well—known stress singularity.

As an alternate to SIMP, a free material optimization was proposed in [21] as a means of addressing the stress singularity in SIMP. Similarly, in [22], binary design variables were used instead of density variables, and the problem was reduced to that of integer-programming, with guaranteed local minima.

Level-Set

The second strategy for solving topology optimization problems relies on defining the evolving topology via a level-set. Since the domain is well-defined at all times, the singularity problem does not arise, and the stiffness matrices are typically well-conditioned. One of the earliest implementation of level-set based stress-constrained topology optimization appears in [23] where the authors proposed to minimize a domain integral of stress subject to material volume constraint. A similar approach was explored in [24]. In particular, to address irregular, i.e., non-rectangular domains, an iso-parametric approach to solving the Hamilton-Jacobi equation was explored by the authors. In the level-set implementation of [8], a new global stress measure was proposed. In [11], [16], the authors combine the advantages of level-set with X-FEM for accurate shape and topology optimization. The active-set methodology with augmented Lagrangian is used to alleviate stress-concentrations.

The authors of [25] were the first to explore the use of topological derivative in stress-based topology optimization. In particular, they introduced a class of penalty functionals for point-wise constraints on the Von Mises stress field. More recently, stress minimization was compared against compliance minimization in [26].

5. Proposed Method

The proposed methodology relies on the concept of topological sensitivity that captures the first order impact of inserting a small circular hole within a domain on various quantities of interest. This concept has its roots in the influential paper by Eschenauer [27], and has later been extended and explored by numerous authors [4], [28]–[31] including generalization to arbitrary features [32]–[34].

To illustrate this concept, consider the structural problem in Figure 1a where an infinitesimal hole of radius r is inserted at point p. Topological sensitivity is defined (in 2D) as the ratio of change in the quantity of interest to the area of the hole, as the hole-size is shrunk to zero, i.e.:

$$\mathcal{T}(p) \equiv \lim_{r \to 0} \frac{Q(r) - Q}{\pi r^2} \tag{3}$$

Various strategies have been proposed to evaluate topological sensitivity; a particularly powerful strategy relates topological sensitivity to shape sensitivity [35]. Specifically, consider the problem posed in Figure 1b where the radius of the hole is controlled through a shape parameter τ. For a fixed radius, one can define shape sensitivity of the quantity of interest with respect to the shape parameter τ as:

$$\chi(r) = \left. \frac{dQ(r)}{d\tau} \right|_{\tau=0} \tag{4}$$

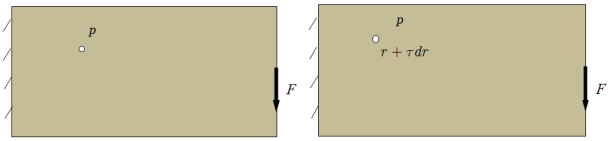

Figure 1: (a) A hypothetical topological change. (b) A hypothetical shape change.

Well-known adjoint methods [36]–[38] can be used to find closed-form expressions for shape-sensitivity (as a function of the radius r). It was then established in [35] that topological derivative as defined in Equation (3) is related to shape sensitivity via:

$$\mathcal{T}(p) = \lim_{r \to 0} \frac{\chi(r)}{2\pi r} \tag{5}$$

Consequently, a closed-form expression for the topological derivative can be derived, and is given in 2D by [4], [28], [29], [31], [39]:

$$\mathcal{T}(p) = \frac{4}{1+\nu}\sigma(u) : \varepsilon(\lambda) - \frac{1-3\nu}{1-\nu^2} tr(\sigma(u)) tr(\varepsilon(\lambda)) \tag{6}$$

where ν is the Poisson ratio, $\sigma(u)$ is the stress field associated with the primary field u, and $\varepsilon(\lambda)$ is the strain field associated with an adjoint field λ that depends on the quantity of interest; see below. Note that the stresses and strains are evaluated at point p in the original domain, i.e., before the hole is inserted.

Given any quantity of interest Q, the adjoint field λ is defined via the linear equation (see [36]):

$$K\lambda = -\nabla_u Q \tag{7}$$

For example, if the quantity of interest is the displacement at the point of force application, then:

$$K\lambda_\delta = -\nabla_u(\delta) = -f / \|f\| \tag{8}$$

Comparing this against $Ku = f$ in Equation (1), it follows that:

$$\lambda_\delta = -u / \|f\| \tag{9}$$

Thus the topological sensitivity for the displacement is given by:

$$\mathcal{T}_\delta(p) = \frac{1}{\|f\|^2}\left[-\frac{4}{1+\nu}\sigma(u) : \varepsilon(u) + \frac{1-3\nu}{1-\nu^2} tr(\sigma(u)) tr(\varepsilon(u))\right] \tag{10}$$

The displacement topological sensitivity (scaled for convenience) is illustrated in Figure 2.

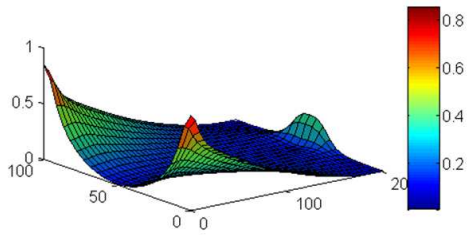

Figure 2: Topological sensitivity field $\mathcal{T}_\delta$

One can similarly compute the topological sensitivity field of maximum von Mises stress (using the p-norm). This is illustrated in Figure 3.

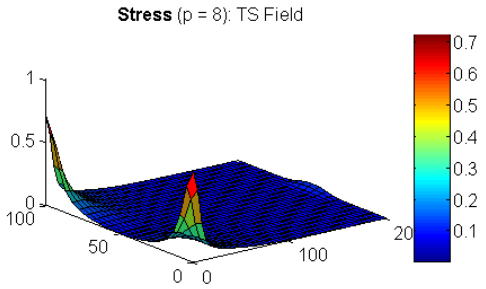

Figure 3: Stress topological sensitivity for $p = 8$.

One can now combine the multiple topological sensitivity fields via:

$$\mathcal{T} = \sum w_i \mathcal{T}_i \tag{11}$$

The weights w_i are determined dynamically depending on the associated constraints. For example, suppose the topology optimization problem involves two displacement constraints:

$$\begin{aligned} \delta_1 &\le \delta_1^{\max} \\ \delta_2 &\le \delta_2^{\max} \end{aligned} \tag{12}$$

Then, the corresponding topological sensitivity fields are combined as follows:

$$\mathcal{T} = \left(\frac{\delta_1}{\delta_1^{\max}}\right)\mathcal{T}_1 + \left(\frac{\delta_2}{\delta_2^{\max}}\right)\mathcal{T}_2 \tag{13}$$

Thus, for example, if at a particular instance $\delta_2 \ll \delta_2^{\max}$, then

$$\mathcal{T} \approx \left(\frac{\delta_1}{\delta_1^{\max}}\right)\mathcal{T}_1 \tag{14}$$

Therefore, only the first topological sensitivity field is active. Now, Figure 4a illustrates the resulting field together with a cutting-plane at an arbitrary height τ. Consider now a domain Ω^τ defined per:

$$\Omega^\tau \equiv \{p \mid \mathcal{T}(p) > \tau\} \tag{15}$$

In other words, the domain Ω^τ is the set of all points where the topological field exceeds τ; the induced domain Ω^τ is illustrated in Figure 4b.

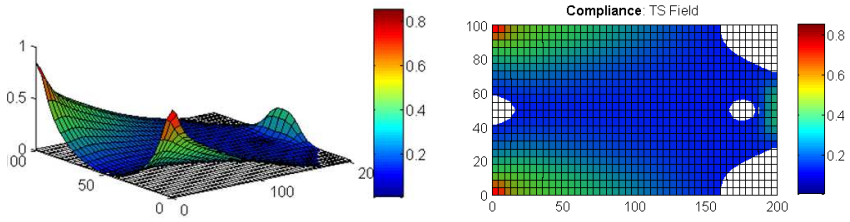

(a) Displacement topological sensitivity. (b) Induced domain Ω^τ

Figure 4: Displacement topological sensitivity field.

However, the computed domain may not be 'pareto-optimal' (see [43]), i.e., it is not the stiffest structure for the given volume fraction. One must now repeat the following three steps: (1) solve the finite element problem over Ω^τ (2) re-compute the topological sensitivity, and (3) find a new value of τ for the desired volume fraction. In essence, we carry out a fixed-point iteration [36], [42], [23] involving three quantities (see Figure 5): (1) domain Ω^τ, (2) displacement fields u and v over Ω^τ, and (3) topological sensitivity field over Ω^τ. Typically, convergence is reached in 3 to 4 iterations [23].

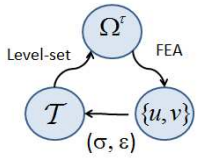

Figure 5: Fixed point iteration involving three quantities

Typically, in finite element analysis (FEA), the global stiffness matrix is assembled prior to a linear-solve. However, in the present work, we have chosen an 'assembly-free' (a.k.a. 'matrix-free') approach [27] where the global stiffness matrix is not assembled or stored. Instead, only the unique individual element stiffness matrices are computed and stored in memory. Not only does this reduce the overall memory requirement (this is especially important for GPU), it can also accelerate topology optimization since FEA is largely memory-bandwidth limited [28].

The primary computational cost of sparse matrix-vector multiplication (SpMV), in today's computational architecture, is memory-access, i.e., floating-point operations are essentially free [2]. In SpMV, there are two types of memory access: (1) accessing elements of the solution vector, and (2) accessing elements of the stiffness matrix. There is very little one can do about the former, except perhaps careful numbering of the mesh nodes. However, the cost of accessing elements of the stiffness matrix can be dramatically reduced through assembly-free methods as discussed below.

Since the geometry is discretized via uniform voxels, all elements are geometrically identical. Therefore all element matrices are identical (barring a 'density' assigned to partial voxels). Thus, one need not assemble or store the global K and M matrices; it is sufficient if a single matrix-pair K_e and M_e is stored.

Consequently, a matrix-free implementation of Kv, for example, may be implemented as follows [19]:

$$Kx = \left(\sum_e K_e\right)x = \sum_e \left(K_e x_e\right) \tag{16}$$

In other words, instead of assembling the K matrix, and then carrying out Kx, we first multiply $K_e x_e$ and then assemble the result.

In the CPU implementation of the assembly-free SpMV, parallelization was attained through OpenMP commands (www.openmp.org). In the GPU implementation using CUDA [20] on NVidia cards, SpMV was implemented by assigning each node of the voxel-grid to a scalar processor. Associated with each voxel node, there are at most 8 voxel elements, and '27' neighboring nodes. When a block of threads are launched, all threads share identical element matrices, and therefore a single memory fetch of the stiffness and mass element matrix per block is sufficient. The three degrees of freedom associated with the 27 nodes are fetched in parallel. In general, during this fetch, it is hard to enforce coalesced memory access for arbitrary voxel-meshes. For more recent GPU cards, we have observed that this is not a serious issue. Finally, many of the low-level operations such as vector-product were implemented using CUBLAS library.

5. Numerical Experiments

In this Section, we present results from numerical experiments. The default parameters are as follows:

- The material properties are $E = 1$ and $\nu = 0.3$.
- In Steps 2 to 5 of the algorithm, the fixed-point iteration is assumed to have converged if the change in maximum displacement is less than 5%.
- The volume step-size set to a maximum value of 0.05.
- Unless otherwise noted, the p-norm value in all experiments is 8.

All experiments were conducted on a Windows 7 64-bit machine with the following hardware:

- Intel I7 960 CPU quad-core running at 3.2GHz with 6 GB of memory; parallelization of CPU code was implemented through OpenMP commands.
- The graphics programmable unit (GPU) is an Nvidia GeForce GTX 480 (480 cores) with 1.5 GB.
- Both the CPU and GPU were configured to run in double-precision.

The topology optimization problem being solved is:

$$\begin{aligned} &\underset{\Omega \subset D}{Min}\, v \\ &\delta \le \delta_{allowed} \\ &\sigma \le \sigma_{allowed} \\ &Ku = f \end{aligned} \tag{17}$$

In all experiments, the displacement and maximum stress constraints are relative to the initial displacement and initial maximum stress, i.e.,

$$\begin{aligned} \delta_{allowed} &= \eta \delta_0 \\ \sigma_{allowed} &= \xi \sigma_0 \end{aligned} \tag{18}$$

The relative values η & ξ are specified for each numerical experiment.

5.1 L-Bracket

The first experiment is on the classic L-Bracket with top load, illustrated in Figure 6.

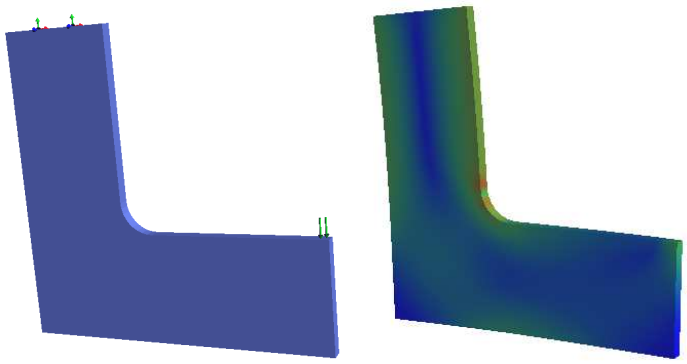

Figure 6: An L-bracket with top load, and resulting deformation.

The geometry was discretized into 8000 elements; Figure 7 illustrates various topologies under differing set of constraints. The CPU and GPU implementations yielded the same topology. The time taken in the CPU implementation, for problem 1, for example, was 140 seconds, while the taken in the GPU implementation was 27 seconds, resulting in a speed-up of 5.2. The speed-up was approximately the same for the other problems.

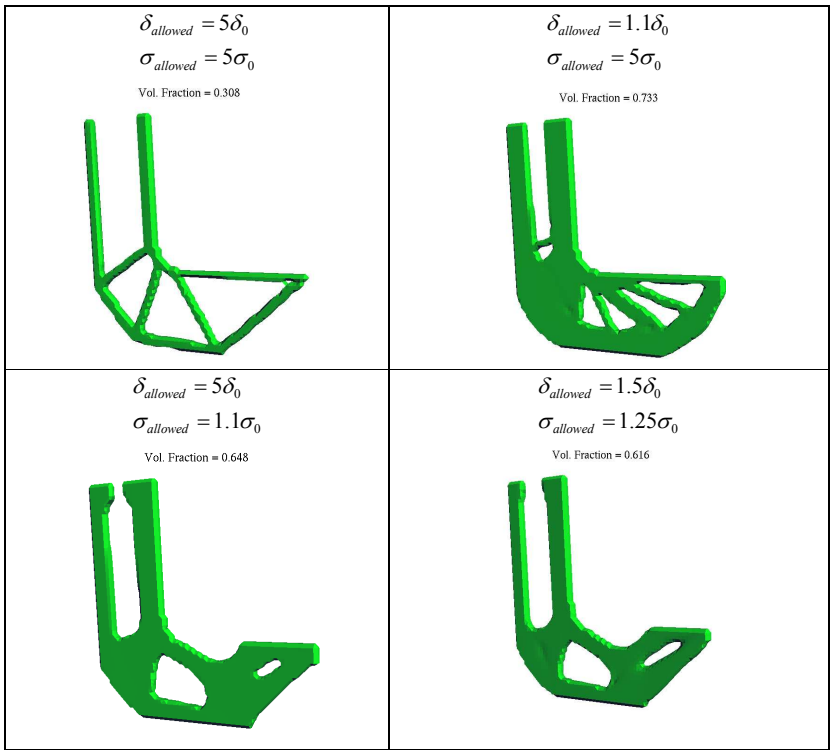

Figure 7: Optimal topologies for various constraints.

5.2. Knuckle problem

The next experiment is on the knuckle problem, illustrated in Figure 8, where two holes are fixed and a vertical force is applied on the third hole at the top; the resulting deformation is also illustrated.

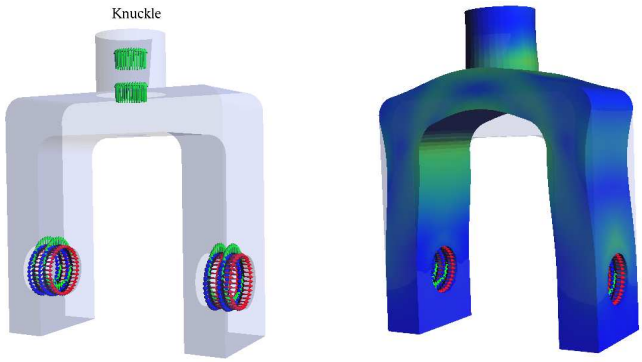

Figure 8: The knuckle problem and resulting deformation.

The geometry was discretized into 70000 elements. Figure 9 illustrates the topologies under two sets of constraints. The time taken in the CPU implementation, for problem 1, for example, was 10 minutes, 11 seconds, while the taken in the GPU implementation was 1 minutes, 3 seconds, resulting in a speed-up of approximately10.

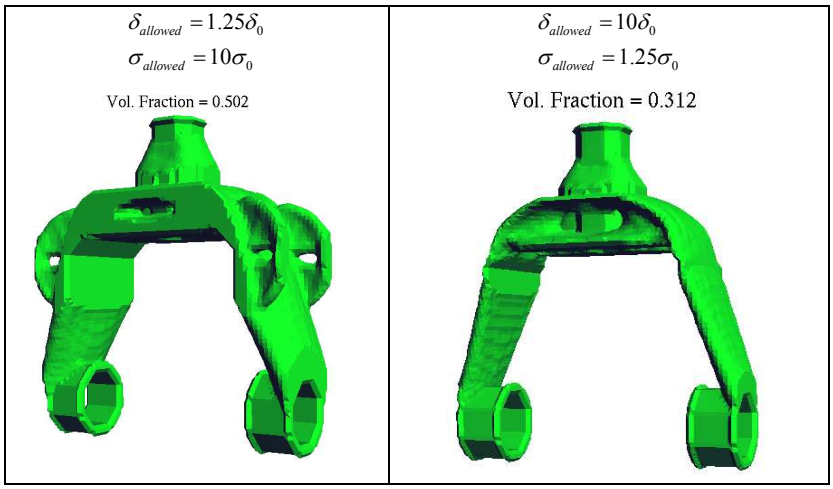

Figure 9: Optimal topologies for the knuckle problem.

6. Conclusions

The main contribution of the paper is a new method for displacement and stress constrained topology optimization. As illustrated via numerical examples, the proposed approach yields both stiff and strong topologies, depending on the constraints. Further, at least one of the two constraints is active at termination. Future work will focus on including other constraints including buckling and eigen-modes. The software will be made available through the author's research website www.ersl.wisc.edu

7. References

[1] G. I. N. Rozvany, "A critical review of established methods of structural topology optimization," *Struct. Multidiscip. Optim.*, vol. 37, no. 3, pp. 217–237, 2009.

[2] M. P. Bendsoe and O. Sigmund, *Topology Optimization: Theory, Methods and Application*, 2nd ed. Springer, 2003.

[3] O. Sigmund, "A 99 line topology optimization code written in Matlab," *Struct. Multidiscip. Optim.*, vol. 21, no. 2, pp. 120–127, 2001.

[4] J. Sokolowski and A. Zochowski, "On Topological Derivative in Shape Optimization," *Siam J. Control Optim.*, vol. 37, no. 4, pp. 1251–1272, 1999.

[5] C. Le, J. A. Norato, T. E. Bruns, C. Ha, and D. A. Tortorelli, "Stress-based topology optimization for continua," *Struct. Multidiscip. Optim.*, vol. 41, no. 4, pp. 605–620, 2010.

[6] J. Paris, F. Navarrina, I. Colominas, and M. Casteleiro, "Topology optimization of continuum structures with local and global stress constraints.," *Struct. Multidiscip. Optim.*, vol. 39, no. 4, pp. 419–437, 2009.

[7] P. Duysinx and M. P. Bendsoe, "Topology optimization of continuum structures with local stress

constraints," *Int J Numer Meth Engng*, vol. 43, no. 8, pp. 1453–1478, 1998.
[8] Q. Xia, T. Shi, S. Liu, and M. Y. Wang, "A level set solution to the stress-based structural shape and topology optimization," *Comput. Struct.*, vol. 90–91, pp. 55–64, 2012.
[9] G. Y. Qiu and X. S. Li, "A note on the derivation of global stress constraints," *Struct. Multidiscip. Optim.*, vol. 40, no. 1–6, pp. 625–628, 2010.
[10] M. Bruggi and P. Duysinx, "Topology optimization for minimum weight with compliance and stress constraints," *Struct. Multidiscip. Optim.*, vol. 46, pp. 369–384, 2012.
[11] W. S. Zhang, X. Guo, M. Y. Wang, and P. Wei, "Optimal topology design of continuum structures with stress concentration alleviation via level set method," *Int. J. Numer. Methods Eng.*, vol. DOI: 10.1002/nme.4416, 2012.
[12] X. Guo and G. D. Cheng, "Epsilon-continuation approach for truss topology optimization," *Acta Mech. Sin.*, vol. 20, no. 5, pp. 526–533, 2004.
[13] C. Le, "Developments in topology and shape optimization," PhD thesis, University of Illinois at Urbana-Champaign, Urbana-Champaign, 2010.
[14] S. Wang, E. D. Sturler, and G. Paulino, "Large-scale topology optimization using preconditioned Krylov subspace methods with recycling," *Int. J. Numer. Methods Eng.*, vol. 69, no. 12, pp. 2441–2468, 2007.
[15] K. Suresh, "Efficient Generation of Large-Scale Pareto-Optimal Topologies**," *Struct. Multidiscip. Optim.*, vol. 47, no. 1, pp. 49–61, 2013.
[16] X. Guo, W. S. Zhang, Y. U. Wang, and P. Wei, "Stress-related topology optimization via level set approach," *Comput Methods Appl Mech Eng*, vol. 200, pp. 3439–3452, 2011.
[17] R. J. Yang and C. J. Chen, "Stress-Based Topology Optimization," *Struct. Optim.*, vol. 12, pp. 98–105, 1996.
[18] F. V. Stump, E. C. N. Silva, and G. Paulino, "Optimization of material distribution in functionally graded structures with stress constraints," *Commun. Numer. Methods Eng.*, vol. 23, no. 6, pp. 535–551, 2007.
[19] M. Bruggi and P. Venini, "A mixed FEM approach to stress constrained topology optimization," *Int. J. Numer. Methods Eng.*, vol. 73, no. 12, pp. 1693–1714, 2008.
[20] V. K. Yalamanchili and A. V. Kumar, "Topology Optimization of Structures using a Global Stress Measure," in *Proceedings of the ASME 2012 International Design Engineering Technical Conferences & Computers and Information in Engineering Conference*, Chicago, IL, 2012.
[21] M. Kocvara and M. Stingl, "Solving stress constrained problems in topology and material optimization," *Struct. Multidiscip. Optim.*, vol. 46, no. 1, pp. 1–15, 2012.
[22] K. Svanberg and M. Werme, "Sequential integer programming methods for stress constrained topology optimization," *Struct. Multidiscip. Optim.*, vol. 34, no. 4, pp. 277–299, 2007.
[23] G. Allaire and F. Jouve, "Minimum stress optimal design with the level set method," *Eng. Anal. Bound. Elem.*, vol. 32, no. 11, pp. 909–918, 2008.
[24] K. A. James, E. Lee, and J. R. R. A. Martins, "Stress-based topology optimization using an isoparametric level set method," *Finite Elem. Anal. Des.*, vol. 58, pp. 20–30, 2012.
[25] S. Amstutz and A. A. Novotny, "Topological optimization of structures subject to Von Mises stress constraints," *Struct. Multidiscip. Optim.*, vol. 41, no. 3, pp. 407–420, 2010.
[26] K. Suresh and M. Takalloozadeh, "Stress-Constrained Topology Optimization: A Topological Level-Set Approach," *Struct. Multidiscip. Optim.*, vol. Submitted, 2012.
[27] H. A. Eschenauer, V. V. Kobelev, and A. Schumacher, "Bubble method for topology and shape optimization of structures," *Struct. Optim.*, vol. 8, pp. 42–51, 1994.
[28] A. A. Novotny, R. A. Feijóo, C. Padra, and E. Taroco, "Topological Derivative for Linear Elastic Plate Bending Problems," *Control Cybern.*, vol. 34, no. 1, pp. 339–361, 2005.
[29] A. A. Novotny, "Topological-Shape Sensitivity Method: Theory and Applications," *Solid Mech. Its Appl.*, vol. 137, pp. 469–478, 2006.
[30] A. A. Novotny, R. A. Feijoo, and E. Taroco, "Topological Sensitivity Analysis for Three-dimensional Linear Elasticity Problem," *Comput. Methods Appl. Mech. Eng.*, vol. 196, no. 41–44, pp. 4354–4364, 2007.
[31] J. Céa, S. Garreau, P. Guillaume, and M. Masmoudi, "The shape and topological optimization connection," *Comput. Methods Appl. Mech. Eng.*, vol. 188, no. 4, pp. 713–726, 2000.
[32] I. Turevsky, S. H. Gopalakrishnan, and K. Suresh, "An Efficient Numerical Method for Computing the Topological Sensitivity of Arbitrary Shaped Features in Plate Bending**," *Int. J. Numer. Methods Eng.*, vol. 79, pp. 1683–1702, 2009.
[33] I. Turevsky and K. Suresh, "Generalization of Topological Sensitivity and its Application to Defeaturing**," in *ASME IDETC Conference*, Las Vegas, 2007.
[34] S. H. Gopalakrishnan and K. Suresh, "Feature Sensitivity: A Generalization of Topological Sensitivity**," *Finite Elem. Anal. Des.*, vol. 44, no. 11, pp. 696–704, 2008.
[35] A. A. Novotny, R. A. Feijoo, E. Taroco, and C. Padra, "Topological Sensitivity Analysis," *Comput. Methods*

Appl. Mech. Eng., vol. 192, no. 7–8Novo03, pp. 803–829, 2003.
[36] K. K. Choi and N. H. Kim, *Structural Sensitivity Analysis and Optimization I: Linear Systems*. New York: Springer, 2005.
[37] D. A. Tortorelli and W. Zixian, "A systematic approach to shape sensitivity analysis," *Int. J. Solids Struct.*, vol. 30, no. 9Tort93, pp. 1181–1212, 1993.
[38] R. A. Feijoo, A. A. Novotny, E. Taroco, and C. Padra, "The topological-shape sensitivity method in two-dimensional linear elasticity topology design," in *Applications of Computational Mechanics in Structures and Fluids*, CIMNE, 2005.
[39] A. A. Novotny, R. A. Feijoo, and E. Taroco, "Topological Sensitivity Analysis for Three-dimensional Linear Elasticity Problem," *Comput. Methods Appl. Mech. Eng.*, vol. 196, no. 41–44, pp. 4354–4364, 2007.
[40] R. T. Shield and W. Prager, "Optimal structural design for given deflection," *J Appl Math Phys*, vol. ZAMP21, pp. 513–523, 1970.